Induction of inclusion formation and disruption of lamin A/C structure by premutation CGG-repeat RNA in human cultured neural cells

Dolores Garcia Arocena[1,2], Christine K. Iwahashi[1], Nelly Won[1], Alexandra Beilina[1], Anna L. Ludwig[1], Flora Tassone[1], Philip H. Schwartz[3] and Paul J. Hagerman[1,*]

[1]Department of Biochemistry and Molecular Medicine, University of California Davis, School of Medicine, Davis, CA 95616, USA, [2]Departamento de Genetica, Facultad de Medicina, UDELAR, Montevideo, Uruguay and [3]Children's Hospital of Orange County Research Institute, Orange, CA 92868, USA

Fragile X-associated tremor/ataxia syndrome (FXTAS) is a neurodegenerative disorder that affects some adult carriers of pre-mutation alleles (55–200 CGG repeats) of the fragile X mental retardation 1 (*FMR1*) gene. FXTAS is thought to be caused by a toxic 'gain-of-function' of the expanded CGG-repeat *FMR1* mRNA, which is found in the neuronal and astrocytic intranuclear inclusions associated with the disorder. Using a reporter construct with a *FMR1* 5′ untranslated region harboring an expanded (premutation) CGG repeat, we have demonstrated that intranuclear inclusions can be formed in both primary neural progenitor cells and established neural cell lines. As with the inclusions found in post-mortem tissue, the inclusions induced by the expanded CGG repeat are αB-crystallin-positive; however, inclusions in culture are not associated with ubiquitin, indicating that incorporation of ubiquitinated proteins is a later event in the disease process. The absence of ubiquitinated proteins also argues against a model in which inclusion formation is due to a failure of the proteasomal degradative machinery. The presence of the expanded CGG repeat, as RNA, results in reduced cell viability as well as the disruption of the normal architecture of lamin A/C within the nucleus. This last observation, and the findings that lamin A/C is present in both the inclusions of FXTAS patients and the inclusions in cell culture, suggests that lamin A/C dysregulation may be a component of the pathogenesis of FXTAS; in particular, the Charcot–Marie–Tooth-type neuropathy associated with FXTAS may represent a functional laminopathy.

INTRODUCTION

Fragile X-associated tremor/ataxia syndrome (FXTAS) is a neurodegenerative disorder that affects many older adults who are carriers of premutation alleles (55–200 CGG repeats) of the fragile X mental retardation 1 (*FMR1*) gene (1–6). It is estimated that at least one-third of males (and a smaller number of females) who harbor premutation alleles will develop FXTAS, suggesting that as many as 1 in 3000–5000 males in the general population may have a lifetime risk of developing FXTAS (7). The core features of FXTAS include progressive intention tremor and/or gait ataxia, with onset typically after 50 years. Ancillary features often include peripheral neuropathy, autonomic dysfunction, parkinsonism and progressive cognitive and behavioral difficulties (memory loss, anxiety, executive deficits) leading to dementia. Characteristic neuroradiological findings include symmetric hyperintensities of the middle cerebellar peduncles (MCPs) on T2-weighted MR imaging (MCP sign) (2,5).

Post-mortem neuropathological examination reveals the presence of ubiquitin-positive, intranuclear inclusions in neurons and astrocytes. Although the inclusions are most abundant in the hippocampus and frontal cortical regions, they are found in broad distribution throughout the brain, brainstem and spinal cord (8,9). The neuropathology of

*To whom correspondence should be addressed at: Department of Biochemistry and Molecular Medicine, University of California Davis, School of Medicine, One Shields Avenue, Davis, CA 95616, USA. Tel: +1 5307547266; Fax: +1 5307547269; Email: pjhagerman@ucdavis.edu

FXTAS also includes white matter disease that is evident in both cerebrum and cerebellum, with cerebellar axonal degeneration and spongiform changes in the deep cerebellar white matter and MCPs (5,8,9).

An important characteristic of FXTAS is that it appears to affect only the carriers of premutation alleles, who have normal or near-normal *FMR1* protein (FMRP) levels in both peripheral blood leucocytes and brain tissue (1,2,4,5,10). Were FXTAS to arise as a consequence of reductions or absence of FMRP, the basis of fragile X syndrome (11), individuals with full mutation alleles ($>$200 CGG repeats) would be the principal population affected by the neurological disorder. Furthermore, levels of the expanded CGG-repeat *FMR1* mRNA are elevated by as much as 5–8-fold in premutation carriers (12–14). These observations, coupled with the fact that the CGG repeat is located in the 5′-untranslated region (5′-UTR) of the *FMR1* message, have led to the hypothesis that FXTAS is the consequence of a toxic 'gain-of-function' of the *FMR1* mRNA itself (1,8,15). In support of this hypothesis, Jin *et al.* (16) demonstrated that expression of the CGG expansion (with a reporter gene) was sufficient to trigger neurodegeneration and inclusion formation in *Drosophila melanogaster*.

The RNA toxicity hypothesis for FXTAS is based on the paradigm established by the myotonic dystrophies, DM1 (*DMPK* gene) and DM2 (*ZNF9* gene) (reviewed in 17–19). A key element of the DM model is that both expanded (CUG)-repeat (*DMPK* or *ZNF9*) mRNAs and protein components are linked to downstream pathogenic mechanisms. If a similar mechanism were operating with FXTAS, examination of the inclusions should reveal both the RNA target and the candidate RNA binding proteins. We have recently verified the first key prediction of this model; namely, the presence of the *FMR1* mRNA in the inclusions (10).

In the current work, we demonstrate that the expanded (CGG)-repeat 5′-UTR in the context of a green fluorescent protein (GFP) reporter plasmid is sufficient to give rise to intranuclear inclusions in two different types of cultured human neural cells, an immortalized line (SK) and primary neural progenitor cells. In addition, transfection with the expanded CGG-repeat plasmid is accompanied by reduced cell viability in a manner that does not appear to require inclusion formation. We have also found that at least two proteins, αB-crystallin (20–23) and lamin A/C (24), in the intranuclear inclusions of FXTAS cases (25), are present in the inclusions formed in cell culture. However, the inclusions in culture do not contain ubiquitin, unlike their counterparts in FXTAS cases (8,25), indicating that the reduced cell viability is not due to the failure of ubiquitin-coupled protein degradation (26–28). Finally, the presence of lamin A/C in the inclusions of FXTAS (25), and the current observation that the lamin A/C nuclear architecture is disrupted in cells transfected with expanded CGG-repeat plasmids, suggests that the neuropathology of FXTAS may be mediated, at least in part, by dysregulation of lamin A/C function. This last possibility would be consistent with the peripheral neuropathy that is common among FXTAS patients.

RESULTS

Intranuclear inclusions form in human neural cells transfected with GFP reporters possessing the FMR1 5′-UTR with 88 CGG repeats

To analyze the effects of expanded CGGs on cultured neural cells, SK cells were transfected with plasmids containing an 88 CGG repeat element in the 5′-UTR of a GFP reporter; mock-transfected cells and cells expressing GFP with a heterologous 5′-UTR under cytomegalovirus (CMV) control were used for comparison. Initial studies were performed using plasmid DNA concentrations ranging from 10 ng to 1 μg per million cells (in 100 μl of mouse astrocyte nucleofector solution/sample) (Table 1). Cells were fixed at 1, 4 and 8 days post-transfection, followed by immunostaining for αB-crystallin, which is a component of FXTAS inclusions (25). No differences in αB-crystallin localization were observed in cells transfected with the lowest concentration (10 ng per million cells) of expanded CGG-repeat plasmid at any of the time points. With either 200 ng or 1 μg of CMV−FMR(CGG)$_{88}$−GFP plasmid per million cells, intranuclear inclusions were observed in at least 2% of nuclei (Fig. 1) at 8 days post-transfection. No inclusions were found in mock-transfected SK cells or in cells expressing CMV−control−GFP. Cell viability was reduced for the highest concentration of plasmid (data not shown). Therefore, the optimal conditions for inclusion formation with the current experimental design were 200 ng plasmid DNA per million cells and analysis at 8 days post-transfection. Staining for αB-crystallin revealed intranuclear inclusions in 5% of the cells expressing the expanded allele (Table 2). Inclusions are generally solitary and intranuclear, as found in FXTAS cases. Interestingly, the percentage of inclusions in the cultured cells is comparable to the values found in post-mortem brain tissue of FXTAS patients (8,9).

The lymphoblastoid cell line (AG), derived from a normal control, was transfected using the optimal conditions mentioned earlier. No inclusions were found at any time point or for any concentration, suggesting that the non-neural lymphoblastoid cells may not support inclusion formation. Nevertheless, cytotoxic effects (decrease in cell viability quantified by flow cytometry of transfected cells stained with propidium iodide) were significantly greater ($P = 0.016$) in lymphoblastoid cells transfected with the highest concentration of CMV−FMR(CGG)$_{88}$−GFP, relative to either mock transfection or transfection with control plasmid. In a separate set of experiments designed to test the effects of CGG repeat size on toxicity, the cell line, AG, was transfected with a series of previously published CMV−FMR(CGG)$_n$−luciferase plasmids ($n = 16$, 30, 62 and 99 CGG repeats) (29). No significant reduction in cell viability was observed in cells expressing 62 or fewer CGG repeats. However, cells expressing 88 CGG repeats suffered a 4-fold reduction in the number of viable cells (200 ng per million cells; 2 days post-transfection) (data not shown).

Antibodies used to detect ubiquitin in the intranuclear inclusions in FXTAS patients (8,25) failed to demonstrate any reactivity to the αB-crystallin inclusions observed in cultured cells transfected with CMV−FMR(CGG)$_{88}$−GFP. The

Table 1. Quantitative analysis of the number of αB-crystallin-positive intranuclear inclusions in neural (SK) cells, induced by different concentrations of CMV−FMR(CGG)$_{88}$−GFP.

DNA concentration (ng/10^6 cells)	CMV−control−GFP			CMV−FMR(CGG)$_{88}$−GFP		
	Number of inclusions	Total cells	%	Number of inclusions	Total cells	%
10	0	400	0	4	400	1
200	0	579	0	23	459	5
1000	0	223	0	4	213	2

Eight days post-transfection.

anti-ubiquitin antibodies did detect perinuclear aggregates in cells expressing the expanded CGG repeat at 8 days; however, the significance of this last observation is not known, as such aggregates are not observed in the cells of FXTAS patients. In the current instance, the absence of co-staining of the inclusions with anti-ubiquitin antibodies suggests that the accumulation of ubiquitinated proteins in the inclusions is a late event in inclusion formation/-maturation (Table 2).

Interestingly, within the first 24 h following transfection, cytoplasmic αB-crystallin aggregates are detected in cells expressing either the expanded CGG or control reporters; however, the aggregates formed during transfection with the control plasmid tend to disappear within 2−3 days post-transfection. These cytoplasmic aggregates persist in nearly one-half of the cells expressing the expanded CGG repeat and are immunopositive for both αB-crystallin and lamin A/C, another protein present within the FXTAS inclusions (25). The significance of these cytoplasmic aggregates is not known; however, they may reflect a redistribution of aggregated material in a dividing cell population.

Intranuclear inclusions are also observed in neural progenitor cells following transfection with the expanded CGG-repeat reporter

To test whether inclusions could be induced in non-immortalized (primary) neural cells of a type that harbors inclusions in FXTAS (8), we transfected primary neural progenitor cells with either the CMV−FMR(CGG)$_{88}$−GFP or CMV−control−GFP reporters under transfection conditions that were found to be optimal for SK cells (200 ng plasmid DNA per million cells). We found that neural cell survival was improved during transfection when the cells were subjected to electroporation in the presence of lymphoblastoid (support) cells in a 1:1 ratio. As the neural progenitor cells, but not the support cells, adhere to the culture flasks, the latter could be removed and discarded with the cell culture medium 24 h post-transfection. As with the SK cells, intranuclear inclusions do form in primary neural cells expressing the CGG expanded repeat allele (Fig. 1), with optimal numbers of inclusions (6%) present at 8 days post-transfection. Again, the number of nuclei harboring inclusions is within the range found for astrocytes in FXTAS cases (8,9).
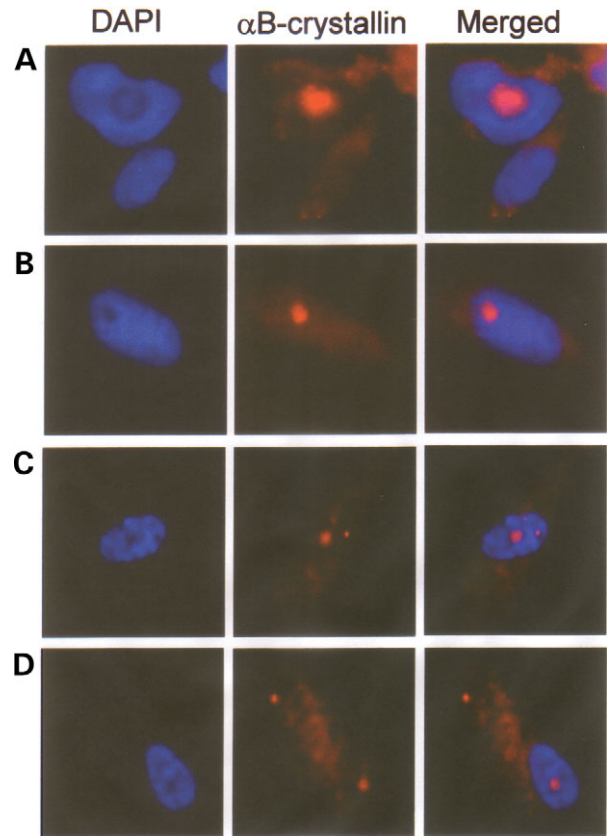

Figure 1. Expression of expanded (premutation) CGG-repeat reporter induces intranuclear inclusion formation in cultured human cells of neural origin. Inclusions were identified by immunostaining for αB-crystallin (red) and counterstaining with DAPI (blue), 8 days post-transfection. Cells were transfected with the CMV−FMR(CGG)$_{88}$−GFP reporter. (**A** and **B**) SK cells; (**C** and **D**) neural progenitor cells. Magnification, 120×.

The expanded CGG repeat as RNA is cytotoxic to neural cells

As noted previously, transfection of neural cells with the expanded CGG-repeat reporter plasmid leads to decreased cell viability; however, this effect could be taking place through mechanisms that are operating either at the DNA or RNA level. To resolve this issue, SK cells were transfected with CMV−FMR(CGG)$_{88}$−GFP, CMV−control−GFP or CMV(del)−FMR(CGG)$_{88}$−GFP (which lacks a functional promoter), followed by incubation with propidium iodide. Fluorescence intensities of GFP, DsRed (transfection control) and propidium iodide were acquired by flow cytometry for 6×10^4 cells per sample. No decreased cell viability was observed in cells transfected with either CMV−control−GFP or CMV(del)−FMR(CGG)$_{88}$−GFP. Thus, the expanded CGG repeat, as DNA, does not contribute to cell toxicity. In contrast, the expanded CGG repeat as RNA transcript led to a significant reduction in cell viability ($P = 0.036$) at 48 h post-transfection with 200 ng per million cells (Fig. 2).

Table 2. Quantitative analysis of inclusion-associated proteins comparing SK cells expressing either CMV−FMR(CGG)$_{88}$−GFP or CMV−control−GFP.

	CMV−control−GFP			CMV−FMR (CGG)$_{88}$−GFP			
	Number	Total cells	%	Number	Total cells	%	*P*-value[a]
Inclusions							
Lamin A/C	0	288	0	6	240	2.5	0.0077
Ubiquitin	0	393	0	0	165	0	na
αB-crystallin	0	579	0	23	459	5	<0.0001
Cytoplasmic aggregates							
Lamin A/C	15	288	5.2	63	240	26.3	<0.0001
Ubiquitin	126	393	32.1	111	165	67.3	<0.0001
αB-crystallin	51	579	8.8	191	459	41.6	<0.0001
lamin A/C							
Rings at nuclear periphery	186	288	64.6	18	240	7.5	<0.0001

200 ng DNA per transfection; analysis performed 8 days post-transfection.
[a]Comparisons of cell numbers/total cells between control and (CGG)$_{88}$ transfections.

Figure 2. Decrease in the percentage of viable SK cells at 2 days post-transfection. Cells were transfected with 200 ng plasmid DNA per million cells for each construct. (C) CMV−control−GFP, (88) CMV−FMR(CGG)88−GFP and (del88) CMV(del)−FMR(CGG)$_{88}$−GFP. Viability (percentage viable cells) was based on propidium iodide exclusion. No significant decrease in cell viability was observed between CMV−control−GFP and the non-expressing CMV(del)−FMR(CGG)$_{88}$−GFP ($P = 0.48$). The reduction in cell viability for CMV−FMR(CGG)88−GFP was significant when compared with either the control ($P = 0.040$) or the inactive, expanded repeat construct ($P = 0.036$).

Reorganization of lamin A/C in the nuclei of neural cells transfected with the expanded CGG-repeat reporter

Lamin A/C is now known to be a component of the intra-nuclear inclusions associated with FXTAS (25). We therefore investigated whether SK cells transfected with CMV−FMR(CGG)$_{88}$−GFP demonstrate any association of lamin A/C-with the induced inclusions. Expression of the expanded CGG-repeat mRNA does lead to the formation of lamin-positive inclusions in ∼2−3% of transfected cells (Table 2). However, a much more striking finding is that expression of the expanded CGG repeat leads to a general disruption of the lamin A/C nuclear architecture, with loss of the uniform ring of lamin A/C at the nuclear perimeter (Fig. 3) and additional dysregulation of lamin A/C within the nuclear matrix. This dysregulation is not present in mock- or control-transfected cells. In contrast, there is no significant difference in the numbers of cells with ring-like organization of lamin B between mock-transfected cells (60/82, 73.2%) and cells expressing CMV−FMR(CGG)$_{88}$−GFP (111/169, 65.7%) (χ^2 $P = 0.213$) (Fig. 3C and D). This last observation suggests that the lamin dysregulation induced by the expanded CGG repeat is relatively specific for the lamin A/C species, consistent with the presence of lamin A/C (24) but not lamin B species, within the inclusions of FXTAS.

Expanded CGGs induce altered nuclear morphology

SK cells transfected with the CMV−FMR(CGG)$_{88}$−GFP construct also display altered nuclear morphology relative to cells expressing the CMV−control−GFP plasmid. In particular, expression of the expanded CGG repeat leads to significant nuclear enlargement, accompanied by greater deviation from a simple spherical shape of the nuclear perimeter (Figs 1
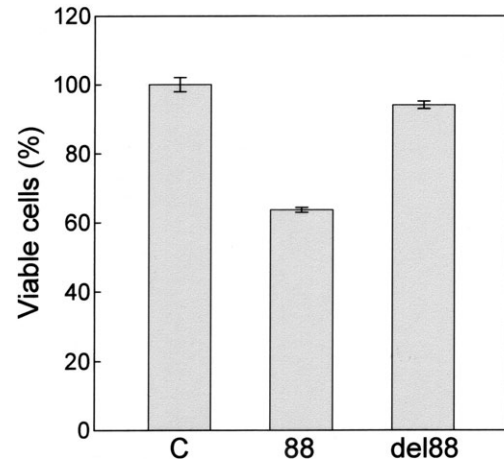
and 3). To quantify these effects, slides containing sorted, transfected SK cells were subjected to laser scanning cytometric analysis. Three nuclear properties were quantified: nuclear area, perimeter (contour length) and nuclear texture; this last property is a measure of the non-uniformity (granularity) of the nuclear matrix as reflected in variations in DAPI staining intensity within a single nucleus.

Cells expressing expanded CGGs have a much broader range of nuclear areas than the control-transfected cells (Fig. 4), with a mean increase of ∼1.6-fold in area (Student's *t*-test, $P = 5.7 \times 10^{-14}$), ∼1.5-fold increase in nuclear perimeter (*t*-test, $P = 2.8 \times 10^{-15}$) and a 3.5-fold increase in texture (*t*-test, $P = 9.9 \times 10^{-28}$), compared with cells expressing control−GFP. The dramatic increase in texture values reflects a more uneven intensity of (DAPI) fluorescence, which corresponds to clumping of nuclear chromatin. We also asked whether the increases in nuclear perimeter were greater than expected for an overall increase in nuclear area (i.e. no change in shape) by comparing the ratio, $r_{p,a}$ = perimeter/(area)$^{1/2}$, between groups (88 CGG repeat versus control). In the absence of any change in nuclear shape between the two groups, $r_{p,a}$ should be the same for both groups; however, we observe a 23% increase in $r_{p,a}$ (*t*-test, $P = 2.0 \times 10^{-10}$) for the nuclei transfected with the 88 CGG-repeat plasmid, suggesting that the shape of the nuclear perimeter is less round for the larger nuclei.

Reduced cell viability associated with the expanded CGG repeat does not appear to be due to apoptotic cell death

The SK cells transfected with CMV−FMR(CGG)$_{88}$−GFP and CMV−control−GFP were analyzed by flow cytometry (MoFlo); viable cells were scored on the basis of propidium
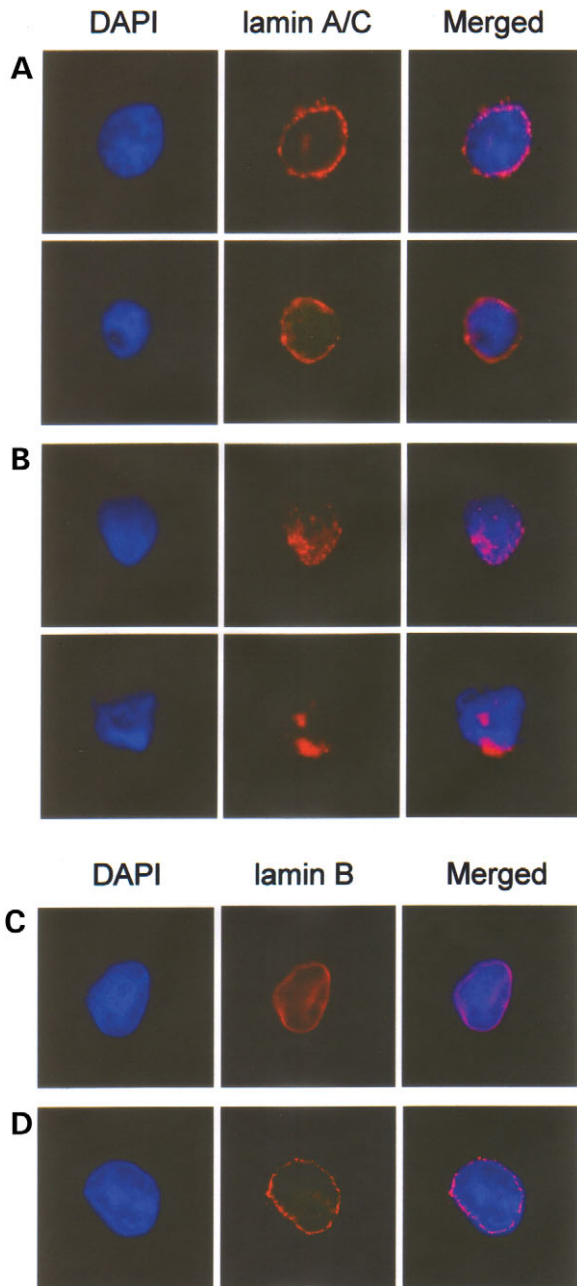
Figure 3. Lamin A/C nuclear architecture is altered in cells that are transfected with the expanded CGG-repeat reporter. (**A**) Normal lamin A/C localization in cells transfected with the CMV−control−GFP reporter. (**B**) Altered lamin A/C organization/aggregation in cells transfected with the CMV−F MR(CGG)$_{88}$−GFP reporter. (**C**) Normal lamin B organization in cells transfected with the CMV−control−GFP reporter. (**D**) Cells transfected with the CMV−FMR(CGG)$_{88}$−GFP reporter. Magnification: 120×, 8 days post-transfection.

iodide exclusion. At 8 days post-transfection, the surviving cell population expressing the expanded CGG repeat is decreased by more than 20-fold relative to the cell population expressing the control−GFP reporter (*t*-test, $P = 4.1 \times 10^{-05}$) or mock-transfected cells (data not shown). To determine whether cell loss was due to apoptotic cell death, cells were subjected to TUNEL assay, which was quantified by

fluorescence microscopy. Cells cultured in the presence of 3 mM camptothecin (positive control for apoptosis) had 25% TUNEL-positive nuclei, whereas cells expressing the expanded CGG repeat had only ∼2% TUNEL-positive nuclei. Control cells (mock-transfected and CMV−control−GFP transfected) had <0.5% TUNEL-positive nuclei. These results suggest that very little of the reduced cell viability is due to apoptotic cell death.

DISCUSSION

A human neural cell model has been developed, which is capable of forming intranuclear inclusions in response to expression of expanded CGG-repeat reporter mRNA. In the current cell culture model, the 5′-UTR of the GFP reporter has been replaced by the *FMR1* 5′-UTR harboring a premutation form of the CGG repeat (88 CGG repeats). The current observations provide further evidence of an RNA-based mechanism for the formation of the intranuclear inclusions of FXTAS because expanded CGG-repeat reporter constructs in which the CMV promoter has been inactivated do not lead to inclusion formation or reduced cell viability. Although the number of cells harboring inclusions is a small percentage of the total number of viable cells, they are comparable to the numbers (∼5%) found in cortical neurons from FXTAS patients (8,9).

The viability of neural cells expressing the expanded CGG repeat is reduced when compared with cells that are either mock-transfected or transfected with control−GFP plasmid. Although the observation of reduced cell viability is consistent with the findings of Handa *et al*. (30), there is no compelling evidence in the current instance that cell loss is due to apoptosis. In terms of the relationship between cell loss and inclusion formation, it is noteworthy that there are greater numbers of inclusions following transfection with lower concentrations of expanded CGG-repeat reporter. However, in the absence of additional studies of the time course of cell loss and/or inclusion formation within individual cells, it is premature to speculate on the potential protective or toxic effects of the inclusions *per se*. Indeed, we cannot rule out that the greater inclusion counts observed for lower concentrations of transfecting DNA may be due to reduced loss of inclusion-bearing cells at earlier times following transfection.

The presence of αB-crystallin within the CGG repeat-induced inclusions is consistent with its presence within the intranuclear inclusions of FXTAS (25) and may reflect an early response to the cellular stress imposed by the expression of the expanded repeat. αB-crystallin is a member of the small heat shock protein (sHsp) family; it is thought to be involved both in the normal dynamics of cytoskeletal proteins (31−35) and in the suppression of protein aggregation during cellular stress (34,36−38). Increased αB-crystallin immunoreactivity is seen in several neurodegenerative conditions, including Alexander's disease, Alzheimer's disease, Parkinson's disease and Creutzfeldt−Jakob disease (22,27). As each condition is characterized by the presence of aggregates of intermediate filaments (IFs) that normally associate with αB-crystallin (33,34,39−41), aggregate formation *per se* may reflect the failure of αB-crystallin to adequately resolve

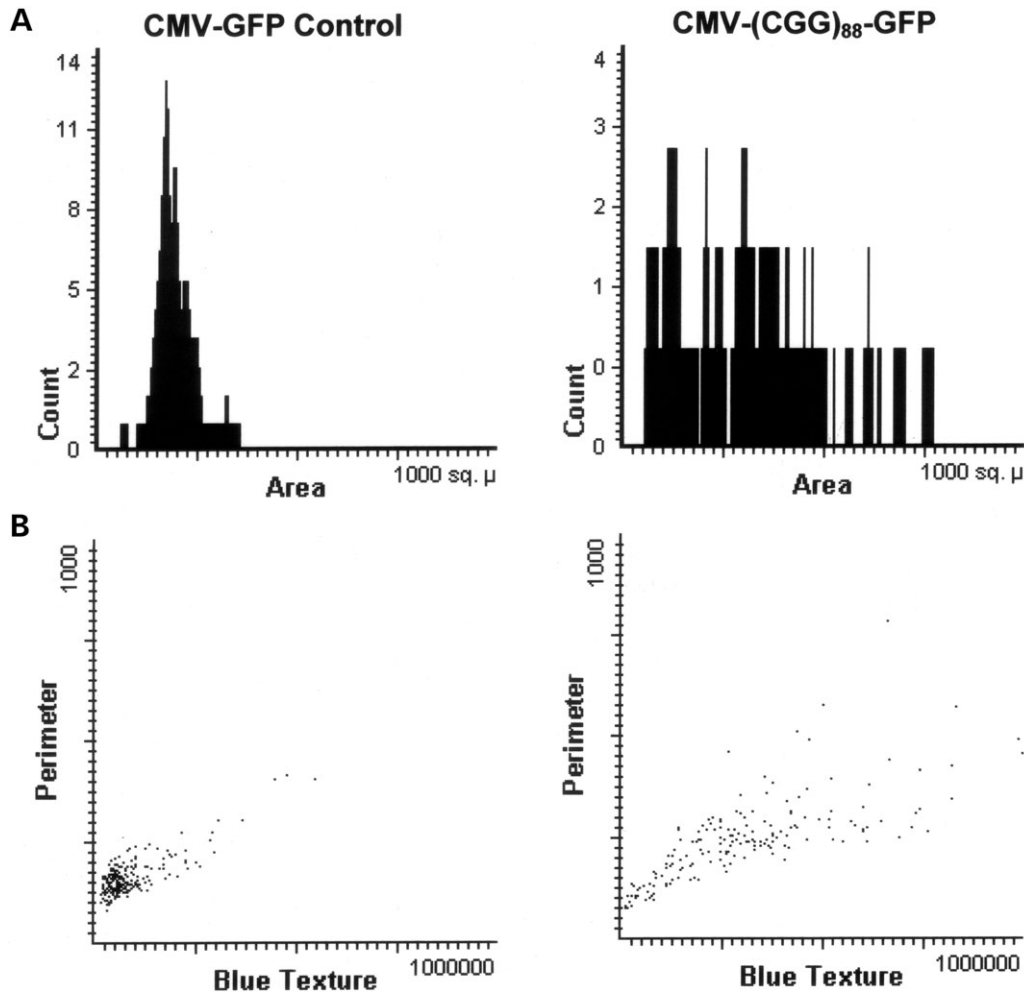**Figure 4.** Laser scanning cytometric comparison of the nuclear morphology of SK cells expressing the control–GFP reporter (305 cells) or the FMR(CGG)$_{88}$–GFP reporter (250 cells). (**A**) Distributions of the nuclear areas of individual cells contoured on the basis of DAPI fluorescence. (**B**) Texture and perimeter of the nuclear areas of individual contoured cells.

the stress-induced disruption of the normal IF architecture in those disorders. Thus, the presence of αB-crystallin within the CGG-repeat-induced inclusions and the inclusions of FXTAS may reflect a similar response to disruption of the normal IF arrangements, in particular, the arrangement of lamin A/C within the nucleoplasm.

No ubiquitin was detected within the αB-crystallin-positive inclusions in SK cells, indicating that inclusion formation induced by the expanded CGG repeat is not a consequence of a failure to adequately degrade ubiquitinated proteins via the proteasomal degradation pathway (42–45). The current observations are consistent with an analysis of the inclusions of FXTAS (25), where the five or six ubiquitinated proteins detected within the inclusions were present only as minor species and none appeared to be polyubiquitinated (i.e. targets for proteasomal degradation). Thus, incorporation of ubiquitin into the inclusions of FXTAS may be a late event in the pathogenesis of the disease.

A possible functional connection between lamin A/C and αB-crystallin was raised by recent experiments of Adhikari *et al.* (35). The investigators suggested that αB-crystallin

might be recruited to mitigate the effects of the stress. They demonstrated that heat shock causes both a substantial increase in the degree of co-localized αB-crystallin and disruption of the ring-like pattern of lamin staining at the nuclear periphery. Thus, in the current context, the expanded CGG repeat itself may provide a local 'stress,' perhaps through its (hypothesized) abnormal recruitment of one or more RNA binding proteins. However, the additional suggestion by Adhikari *et al.* (35) and others (46,47), namely that αB-crystallin and lamin A/C co-localize within splicing factor compartments (nuclear speckles), has been called into question by the recent demonstration of Večeřová *et al.* (48) that the earlier immunocytochemical studies used an antibody that was likely to be detecting non-lamin A/C epitopes (48).

Expression of the expanded CGG-repeat RNA in cultured SK cells also results in the accumulation of lamin A/C within the intranuclear inclusions. This finding is in accord with the observation that lamin A/C is present within the neural cell intranuclear inclusions of FXTAS patients (25). Furthermore, the expanded-repeat RNA leads to the disruption of the normal ring-like arrangement of lamin A/C at the

nuclear periphery, with a nearly 9-fold reduction in the number of cells with the ring-like morphology. This second aspect of the altered distribution of lamin A/C, with associated changes in nuclear morphology (e.g. increased nuclear volume), is far more widespread than the formation of inclusions *per se* and therefore may be of more importance to disease pathogenesis and cell death.

Both the redistribution of lamin A/C to the intranuclear inclusions and the disruption of the ring-like distribution of lamin A/C are strikingly similar to the abnormal lamin A/C distribution observed with mutant forms of lamin A/C (*LMNA* gene; OMIM 150330) associated with several of the human laminopathies (49,50). At least four lamin A/C mutations (N195K, E358K, M371K, R386K) expressed in mouse myoblasts lead to the formation of intranuclear aggregates and loss of lamin A/C staining at the nuclear rim (51). Similar observations have been made with HeLa cells transfected with the N195K mutant (52) and with CHO-K1 cells transfected with three additional lamin A/C mutants [R386K and R453W, causing Emory–Dreifuss muscular dystrophy (EDMD); R482W, causing familial partial lipodystrophy] (46). Moreover, Lammerding *et al.* (47) observed increasing deformation of the nuclear periphery in *LMNA* −/− mice, also consistent with the current observations.

The influence of *LMNA* mutations on the nuclear organization of A or B type lamins appears to depend on the location of the mutation within the lamin A/C coding sequence (51,53). For example, Reichart *et al.* (53) recently found that *LMNA* mutation R377H, responsible for AD-EDMD, does not influence lamin B2 organization at the nuclear periphery, similar to our current observations in which lamin A/C disruption is not accompanied by altered lamin B organization.

In addition to the close parallel between the morphological changes induced by expression of the expanded CGG repeat and the histopathology of some disease-forming *LMNA* mutations (intranuclear foci/inclusions, loss of lamin A/C from the nuclear periphery, nuclear enlargement/distortion), there exist parallels at the clinical level between the FXTAS and the laminopathies (50,54,55). In particular, a specific mutation (R298C) in the *LMNA* gene causes an axonal (type 2), autosomal recessive form of Charcot–Marie–Tooth (CMT) disease, designated CMT2B1 (OMIM no. 605588) (55–57). Features of a CMT type 2 neuropathy are present in most FXTAS patients. All five subjects of the original report of FXTAS had signs of peripheral (lower distal extremity) neuropathy (1). In a follow-up study, 60% (12/20) of subjects had peripheral neuropathy (abolished reflexes, loss of vibration sense) on neurological exam (5). In the latter study, four patients had undergone nerve conduction studies, and nerve conduction velocities were mildly but clearly reduced in all four cases, consistent with an axonal (CMT type 2) neuropathy. We have since seen two patients in clinic (unpublished data) who had received a prior diagnosis of CMT, but were subsequently determined to have FXTAS. However, it is not known whether the mutation (R298C) giving rise to the CMT2B1 phenotype results in any altered organization of lamin A/C within the nuclei of affected cells. Finally, it is interesting to note that single point mutations within the *LMNA* gene (e.g. R298C, with CMT2B1) can lead to broad variation in the clinical phenotype, even within single families (58). This variable penetrance is also a characteristic of the clinical presentation in FXTAS (7).

CONCLUSION

We have demonstrated that an expanded CGG-repeat element, when transcribed, causes the induction of intranuclear inclusions in both immortalized (SK) and primary human neural progenitor cells in culture; transcripts containing the non-coding, expanded repeat element are also cytotoxic to both cell types. The inclusions contain αB-crystallin and lamin A/C, both present in the inclusions of FXTAS (25); however, the inclusions are ubiquitin-negative, suggesting that incorporation of ubiquitin proteins is a later stage of inclusion formation in the disease process.

A significant clinical feature of FXTAS is a peripheral (axonal) neuropathy that is similar to a form of type 2 CMT that is caused by mutations in the *LMNA* gene. On the basis of our current and previous findings, we hypothesize that FXTAS may represent a functional laminopathy; that is, abnormal lamin A/C function, induced by the expanded CGG repeat RNA, leads to many of the downstream effects involving both CNS and peripheral nerve pathology. Because the proposed lamin A/C dysfunction is not due to a single mutant form of *LMNA*, the dysfunction in FXTAS may result in a mixed lamin A/C phenotype. In this regard, we do see FXTAS cases with cardiac conduction defects as well as bulbar signs (e.g. difficulty in swallowing) (unpublished data), both features of other laminopathies (59). Adding to the potential for a mixed CMT phenotype, another sHsp found within the inclusions of FXTAS, Hsp27, is also responsible for a form of axonal CMT (CMT2F) (60).

On the basis of the role of αB-crystallin in organizing IFs, its recruitment to the nucleus in response to cellular stress, its co-localization with lamin A/C in the nucleus and the redistribution of lamin A/C in response to stress and/or specific *LMNA* mutations, we hypothesize further that the CGG repeat *per se* acts as the initial stressor, perhaps due to altered binding of proteins that are involved with co-transcriptional or post-transcriptional mRNA processing. Indeed, lamin A/C is known to be involved in both DNA replication and transcription through its interactions with numerous transcriptional mediators (61–63). The αB-crystallin response may be either due to the abnormal CGG–protein complex or due to some feature of the altered IF architecture within the nucleus.

The current cell model for inclusion formation will facilitate the dissection of the pathway from the initial expression of the expanded CGG repeat to the neurotoxicity and cell death that is undoubtedly responsible for the white matter disease and global brain atrophy observed in FXTAS.

MATERIALS AND METHODS

Plasmids

CMV–control–GFP is identical to pEGFP-N1 (Clontech, BD Biosciences, CA, USA), which encodes a variant of the wild-type GFP, driven by a human CMV promoter that has been optimized for expression in mammalian cells.

CMV-DsRed2-N1 (Clontech, BD Biosciences) encodes a DsRed variant that is optimized for high expression in transfected mammalian cells. Expression of this reporter can be monitored by flow cytometry and was used as a transfection marker.

CMV−FMR(CGG)$_{88}$−GFP consists of a pEGFP-N1 backbone, into which has been inserted (between multiple cloning sites *Pst*I and *Nco*I) the 5′-UTR region of the *FMR1* gene (*Pst*I−*Nco*I fragment) harboring a 88 CGG repeat allele. The *Pst*I−*Nco*I fragment was derived from pCMV-(CGG)$_{99}$-FL (64). It should be noted that resizing of the CGG repeat yielded a somewhat lower number (88 CGG repeats) than cited in the earlier study.

CMV(del)−FMR(CGG)$_{88}$−GFP was obtained by deleting the entire CMV promoter region (*Bgl*II−*Hin*dIII fragment) from CMV−FMR(CGG)$_{88}$−GFP. The absence of expression in transfected cells was confirmed by fluorescent flow cytometry.

Plasmids were checked by restriction digestion to confirm CGG repeat stability following cloning and Endofree maxiprep plasmid purification (Qiagen, CA, USA), as described (29). Briefly, plasmid DNAs were digested with *Blp*I/*Nhe*I and the fragments containing the CGG repeats were purified and loaded on a denaturing high resolution polyacrylamide gel together with molecular weight markers. Allele sizes were determined using FluorChem 8800 software (Alpha Innotech Corp., San Leandro, CA, USA). The CGG expansion size is 88 ± 2 CGG repeats.

Cell culture

Human neurally derived SK-N-MC cells (30 and 40 CGG repeat *FMR1* alleles) (ATCC, WA, USA) were maintained in Dulbecco's modified Eagle medium without phenol red (GIBCO, NY, USA), supplemented with 10% fetal bovine serum (GIBCO) and 1× antibiotic−antimycotic solution (penicillin-G, streptomycin solution, amphotericin-B) (Gemini Bio-Products, CA, USA).

Neural progenitor cells from a normal female (SC007; 28 and 32 CGG-repeat *FMR1* alleles) were isolated from the periventricular zone in the area of the head of the caudate nucleus regions, as previously described (65). The primary culture was maintained in HAM's F-12 DME high glucose without L-glutamine (Irvine Scientific, CA, USA) and supplemented with 20% fetal calf serum.

Human lymphoblastoid cell line AG09391 (AG) (NIA Cell Repositories, NJ, USA), derived from a normal female (16 and 29 CGG-repeat *FMR1* alleles), was maintained in RPMI medium 1640 without phenol red (GIBCO), supplemented with 10% fetal bovine serum (GIBCO) and 1× antibiotic−antimycotic solution (penicillin-G, streptomycin solution, amphotericin-B) (Gemini Bio-Products).

Cell lines were genotyped for CGG number by PCR as described (66).

Transient transfection

Cultured cells in their exponential growth phase were detached with 13 µl/cm^2 trypsin−EDTA (GIBCO). SK cells were transfected with 10, 200 or 1000 ng of CMV−control−GFP or CMV−FMR(CGG)$_{88}$−GFP per million cells, using 100 µl of mouse astrocyte nucleofector solution/sample (Amaxa, MD, USA). The toxic effect of the expanded *FMR1* CGG element was analyzed by transfecting SK cells with 200 ng per million cells of CMV−control−GFP, CMV−FMR(CGG)$_{88}$−GFP or CMV(del)−FMR(CGG)$_{88}$−GFP; all transfection reactions were co-transfected with 100 ng per million cells of CMV-DsRed2-N1 as a transfection control.

Neural progenitor cells were transfected with 200 or 1000 ng of CMV−control−GFP or CMV−FMR(CGG)$_{88}$−GFP per million cells, using mouse astrocyte nucleofector solution (Amaxa). Cells were plated at a density of $1 \times 10^5/\text{cm}^2$ and incubated at 37°C, 5% CO$_2$. All samples were run at least in triplicate.

Selection of transformed cells

Ten million cells per sample were dissociated following incubation with 13 µl/cm^2 Trypsin−EDTA (1×) (GIBCO) for 5 min at 37°C and were resuspended in 500 µl Dulbecco's phosphate-buffered saline solution (GIBCO). Cells were filtered using a cell-strainer (Falcon, CA, USA), and 15 µl of propidium iodide (50 µg/ml) was added to each sample; the resulting suspension was incubated for 15 min at room temperature. Populations of viable cells expressing the reporter genes were recovered in 1 ml of fetal bovine serum (GIBCO) by gating propidium iodide-negative (viable) and GFP-positive single cells in a high speed MoFlo cell sorter (Cytomation, CO, USA). Fluors were excited by an Enterprise laser (Coherent, CA, USA), providing a 488 nm excitation wavelength (EGFP and propidium iodide have emission maxima of 507 and 617 nm, respectively). Multicolor analyses of at least three replicates, each consisting of 2.0×10^4 cells, were acquired using Summit software (Cytomation) and analyzed using FloJo software (Treestar Inc., CA, USA).

Immunofluorescence staining

Initial immunofluorescence studies were performed on non-sorted SK cells at 3 h and 1, 4, 8 and 16 days post-transfection. Subsequent immunofluorescence experiments were performed on sorted cells. Sorted cells were either grown on Permanox 4 chamber slides (Nalge Nunc International, NY, USA) at a cell density of 3×10^4 per chamber in 1 ml of appropriate culture media or spun from the cell suspension recovered by the cell sorter onto Superfrost Plus microscope slides (Fisher Scientific, PA, USA) at 1000 r.p.m. for 8 min at room temperature using a Cytofuge 2 (StatSpin, MA, USA). At selected time points following transfection, slides were fixed in Histochoice (Amresco, OH, USA) for 10 min, followed by three washes in PBS-T (10 mM sodium phosphate, 150 mM sodium chloride, pH 7.4, 0.1% polyethylene 20 sorbitan monolaurate) for 5 min each at room temperature.

Non-specific binding sites were blocked with 5% goat serum in PBS-T for 2 h. Slides were incubated overnight at 4°C with primary antibodies diluted 1:500 in blocking solution: rabbit polyclonal anti-ubiquitin (Novus Biologicals, CO, USA); mouse monoclonal anti-ubiquitin (AbCam, MA, USA); mouse monoclonal anti-αB-crystallin (Stressgen,

Canada); goat polyclonal anti-lamin B (M-20) (Santa Cruz Biotechnology, CA, USA), which detects lamin B1, and to a lesser extent, lamin B2 and B3 (referred to collectively as lamin B); mouse monoclonal anti-lamin A/C (BD Transduction Laboratories, CA, USA), which recognizes both lamin A and C isoforms by 1D western blot (data not shown). Slides were washed extensively and incubated with 1:500 (v/v) Alexa 555 labeled goat anti-mouse IgG (Invitrogen Molecular Probes, OH, USA) or with Cy3 labeled donkey anti-goat (Jackson Immuno Research, PA, USA) for lamin B, for 2 h at 20°C. Nuclei were stained with 2 μM DAPI (4′, 6-diamidino-2-phenyindole di-lactate). Slides were mounted with coverslips in the presence of ProLong mounting media (Invitrogen).

Neural progenitor and SK nuclei, as well as fluorescent stained proteins, were counted manually in multiple fields of triplicate slides at 100× magnification using an Axioplan 2 fluorescent microscope (Zeiss, Germany). Images were acquired using IP Lab software (Scanalytics Inc., VA, USA).

Laser scanning cytometry

The nuclear morphology of sorted cells, immunostained with anti-lamin A/C antibody and counterstained with DAPI, was quantified using a laser scanning cytometer (LSC-1) (Compu-Cyte, MA, USA). Slides were scanned on an LSC-1 under a 20× objective. Cells expressing CMV–control–GFP or CMV–FMR(CGG)$_{88}$–GFP were excited with a 480 nm argon laser and their nuclei were contoured on the basis of nuclear (DAPI) fluorescence. Cell clusters were excluded from the analysis by gating as described (67). The area, perimeter and texture of the DAPI-stained nuclei were determined for at least 250 cells per sample; analysis was performed using Wincyte software (CompuCyte). The area is defined as the number of pixels inside the contour of the nuclei; the perimeter is defined as the distance around the nuclei. The texture is defined as the variability of fluorescence intensity in the nuclei (higher texture values reflect coarse chromatin texture, whereas lower values reflect fine chromatin texture).

TUNEL assay

The extent of apoptotic cell death was analyzed in cells transfected with either CMV–control–GFP or CMV–FMR(CGG)$_{88}$–GFP, using an *in situ* cell death detection kit (Roche, IN, USA), following the manufacturer's instructions. Positive controls for apoptosis consisted of cells cultured in the presence of 3 mM camptothecin (Sigma-Aldrich, MO, USA), incubated for 24 h at 37°C. Controls for cell autofluorescence and negative controls were included, as suggested by the manufacturer. The degree of labeling of DNA strand breaks and alterations in cell morphology following DAPI staining were evaluated and quantified by fluorescence microscopy using an excitation wavelength of 515 nm. Systematic viability assays to quantify cell survival were considered beyond the scope of this work; such studies are in progress (unpublished data).

REFERENCES

1. Hagerman, R.J., Leehey, M., Heinrichs, W., Tassone, F., Wilson, R., Hills, J., Grigsby, J., Gage, B. and Hagerman, P.J. (2001) Intention tremor, parkinsonism, and generalized brain atrophy in male carriers of fragile X. *Neurology*, **57**, 127–130.
2. Brunberg, J.A., Jacquemont, S., Hagerman, R.J., Berry-Kravis, E.M., Grigsby, J., Leehey, M.A., Tassone, F., Brown, W.T., Greco, C.M. and Hagerman, P.J. (2002) Fragile X premutation carriers: characteristic MR imaging findings of adult male patients with progressive cerebellar and cognitive dysfunction. *Am. J. Neuroradiol.*, **23**, 1757–1766.
3. Leehey, M.A., Munhoz, R.P., Lang, A.E., Brunberg, J.A., Grigsby, J., Greco, C., Jacquemont, S., Tassone, F., Lozano, A.M., Hagerman, P.J. *et al.* (2003) The fragile X premutation presenting as essential tremor. *Arch. Neurol.*, **60**, 117–121.
4. Berry-Kravis, E., Lewin, F., Wuu, J., Leehey, M., Hagerman, R., Hagerman, P. and Goetz, C.G. (2003) Tremor and ataxia in fragile X premutation carriers: blinded videotape study. *Ann. Neurol.*, **53**, 616–623.
5. Jacquemont, S., Hagerman, R.J., Leehey, M., Grigsby, J., Zhang, L., Brunberg, J.A., Greco, C., Des Portes, V., Jardini, T., Levine, R. *et al.* (2003) Fragile X premutation tremor/ataxia syndrome: molecular, clinical, and neuroimaging correlates. *Am. J. Hum. Genet.*, **72**, 869–878.
6. Jacquemont, S., Farzin, F., Hall, D., Leehey, M., Tassone, F., Gane, L., Zhang, L., Grigsby, J., Jardini, T., Lewin, F. *et al.* (2004) Aging in individuals with the *FMR1* mutation. *Am. J. Ment. Retard.*, **109**, 154–164.
7. Jacquemont, S., Hagerman, R.J., Leehey, M.A., Hall, D.A., Levine, R.A., Brunberg, J.A., Zhang, L., Jardini, T., Gane, L.W., Harris, S.W. *et al.* (2004) Penetrance of the fragile X-associated tremor/ataxia syndrome in a premutation carrier population. *JAMA*, **291**, 460–469.
8. Greco, C.M., Hagerman, R.J., Tassone, F., Chudley, A.E., Del Bigio, M.R., Jacquemont, S., Leehey, M. and Hagerman, P.J. (2002) Neuronal intranuclear inclusions in a new cerebellar tremor/ataxia syndrome among fragile X carriers. *Brain*, **125**, 1760–1771.
9. Greco, C., Berman, R., Martin, R., Tassone, F., Schwartz, P., Brunberg, J., Grigsby, J., Hessl, D., Becker, E., Papazian, J. *et al.* (2005) Neuropathology of fragile X-associated tremor/ataxia syndrome (FXTAS). *Brain*, in press.
10. Tassone, F., Iwahashi, C. and Hagerman, P.J. (2004) *FMR1* RNA within the intranuclear inclusions of fragile X-associated tremor/ataxia syndrome (FXTAS). *RNA Biol.*, **1**, 103–105.
11. Hagerman, R.J. and Hagerman, P.J. (eds) (2002) *Fragile X Syndrome: Diagnosis, Treatment, and Research.* 3rd edn, The Johns Hopkins University Press, Baltimore.
12. Tassone, F., Hagerman, R.J., Taylor, A.K., Gane, L.W., Godfrey, T.E. and Hagerman, P.J. (2000) Elevated levels of *FMR1* mRNA in carrier males: a new mechanism of involvement in fragile X syndrome. *Am. J. Hum. Genet.*, **66**, 6–15.
13. Tassone, F., Hagerman, R.J., Chamberlain, W.D. and Hagerman, P.J. (2000) Transcription of the *FMR1* gene in individuals with fragile X syndrome. *Am. J. Med. Genet.*, **97**, 195–203.
14. Kenneson, A., Zhang, F., Hagedorn, C.H. and Warren, S.T. (2001) Reduced FMRP and increased *FMR1* transcription is proportionally associated with CGG repeat number in intermediate-length and premutation carriers. *Hum. Mol. Genet.*, **10**, 1449–1454.

15. Hagerman, P.J. and Hagerman, R.J. (2004) Fragile X-associated tremor/ataxia syndrome (FXTAS). *Ment. Retard. Dev. Disabil. Res. Rev.*, **10**, 25–30.

16. Jin, P., Zarnescu, D.C., Zhang, F., Pearson, C.E., Lucchesi, J.C., Moses, K. and Warren, S.T. (2003) RNA-mediated neurodegeneration caused by the fragile X premutation rCGG repeats in *Drosophila*. *Neuron*, **39**, 739–747.

17. Finsterer, J. (2002) Myotonic dystrophy type 2. *Eur. J. Neurol.*, **9**, 441–447.

18. Mankodi, A. and Thornton, C.A. (2002) Myotonic syndromes. *Curr. Opin. Neurol.*, **15**, 545–552.

19. Ranum, L.P. and Day, J.W. (2004) Myotonic dystrophy: RNA pathogenesis comes into focus. *Am. J. Hum. Genet.*, **74**, 793–804. Epub 2004 April 2002.

20. Gordon, N. (2003) Alexander disease. *Eur. J. Paediatr. Neurol.*, **7**, 395–399.

21. Gai, W.P., Power, J.H., Blumbergs, P.C., Culvenor, J.G. and Jensen, P.H. (1999) Alpha-synuclein immunoisolation of glial inclusions from multiple system atrophy brain tissue reveals multiprotein components. *J. Neurochem.*, **73**, 2093–2100.

22. Dabir, D.V., Trojanowski, J.Q., Richter-Landsberg, C., Lee, V.M. and Forman, M.S. (2004) Expression of the small heat-shock protein alphaB-crystallin in tauopathies with glial pathology. *Am. J. Pathol.*, **164**, 155–166.

23. den Engelsman, J., Bennink, E.J., Doerwald, L., Onnekink, C., Wunderink, L., Andley, U.P., Kato, K., de Jong, W.W. and Boelens, W.C. (2004) Mimicking phosphorylation of the small heat-shock protein alphaB-crystallin recruits the F-box protein FBX4 to nuclear SC35 speckles. *Eur. J. Biochem.*, **271**, 4195–4203.

24. Hutchison, C.J. and Worman, H.J. (2004) A-type lamins: guardians of the soma? *Nat. Cell Biol.*, **6**, 1062–1067.

25. Iwahashi, C.K., Yasui, D.H., An, H.-J., Greco, C.M., Tassone, F., Nannen, K., Babineau, B., Lebrilla, C.B., Hagerman, R.J. and Hagerman, P.J. (2005) Protein composition of the intranuclear inclusions of FXTAS. *Brain, Advanced Access* doi:10.1093/brain/awh1650.

26. Kaytor, M.D. and Warren, S.T. (1999) Aberrant protein deposition and neurological disease. *J. Biol. Chem.*, **274**, 37507–37510.

27. Sherman, M.Y. and Goldberg, A.L. (2001) Cellular defenses against unfolded proteins: a cell biologist thinks about neurodegenerative diseases. *Neuron*, **29**, 15–32.

28. Garcia-Mata, R., Gao, Y.S. and Sztul, E. (2002) Hassles with taking out the garbage: aggravating aggresomes. *Traffic*, **3**, 388–396.

29. Chen, L.S., Tassone, F., Sahota, P. and Hagerman, P.J. (2003) The (CGG)n repeat element within the 5′ untranslated region of the *FMR1* message provides both positive and negative *cis* effects on *in vivo* translation of a downstream reporter. *Hum. Mol. Genet.*, **12**, 3067–3074.

30. Handa, V., Goldwater, D., Stiles, D., Cam, M., Poy, G., Kumari, D. and Usdin, K. (2005) Long CGG-repeat tracts are toxic to human cells: implications for carriers of Fragile X premutation alleles. *FEBS Lett.*, **579**, 2702–2708.

31. van de Klundert, F.A., Gijsen, M.L., van den, I.P.R., Snoeckx, L.H. and de Jong, W.W. (1998) alpha B-crystallin and hsp25 in neonatal cardiac cells—differences in cellular localization under stress conditions. *Eur. J. Cell Biol.*, **75**, 38–45.

32. Perng, M.D., Cairns, L., van den, I.P., Prescott, A., Hutcheson, A.M. and Quinlan, R.A. (1999) Intermediate filament interactions can be altered by HSP27 and alphaB-crystallin. *J. Cell Sci.*, **112**, 2099–2112.

33. Perng, M.D., Muchowski, P.J., van Den, I.P., Wu, G.J., Hutcheson, A.M., Clark, J.I. and Quinlan, R.A. (1999) The cardiomyopathy and lens cataract mutation in alphaB-crystallin alters its protein structure, chaperone activity, and interaction with intermediate filaments *in vitro*. *J. Biol. Chem.*, **274**, 33235–33243.

34. Head, M.W. and Goldman, J.E. (2000) Small heat shock proteins, the cytoskeleton, and inclusion body formation. *Neuropathol. Appl. Neurobiol.*, **26**, 304–312.

35. Adhikari, A.S., Sridhar Rao, K., Rangaraj, N., Parnaik, V.K. and Mohan Rao, C. (2004) Heat stress-induced localization of small heat shock proteins in mouse myoblasts: intranuclear lamin A/C speckles as target for alphaB-crystallin and Hsp25. *Exp. Cell Res.*, **299**, 393–403.

36. Narberhaus, F. (2002) Alpha-crystallin-type heat shock proteins: socializing minichaperones in the context of a multichaperone network. *Microbiol. Mol. Biol. Rev.*, **66**, 64–93.

37. Djabali, K., Piron, G., de Nechaud, B. and Portier, M.M. (1999) alphaB-crystallin interacts with cytoplasmic intermediate filament bundles during mitosis. *Exp. Cell Res.*, **253**, 649–662.

38. Salvador-Silva, M., Ricard, C.S., Agapova, O.A., Yang, P. and Hernandez, M.R. (2001) Expression of small heat shock proteins and intermediate filaments in the human optic nerve head astrocytes exposed to elevated hydrostatic pressure *in vitro*. *J. Neurosci. Res.*, **66**, 59–73.

39. Lowe, J., McDermott, H., Pike, I., Spendlove, I., Landon, M. and Mayer, R.J. (1992) Alpha B crystallin expression in non-lenticular tissues and selective presence in ubiquitinated inclusion bodies in human disease. *J. Pathol.*, **166**, 61–68.

40. Wisniewski, T. and Goldman, J.E. (1998) Alpha B-crystallin is associated with intermediate filaments in astrocytoma cells. *Neurochem. Res.*, **23**, 385–392.

41. Horwitz, J. (1992) Alpha-crystallin can function as a molecular chaperone. *Proc. Natl Acad. Sci USA*, **89**, 10449–10453.

42. Johnston, J.A., Ward, C.L. and Kopito, R.R. (1998) Aggresomes: a cellular response to misfolded proteins. *J. Cell Biol.*, **143**, 1883–1898.

43. Chung, K.K., Dawson, V.L. and Dawson, T.M. (2001) The role of the ubiquitin–proteasomal pathway in Parkinson's disease and other neurodegenerative disorders. *Trends. Neurosci.*, **24**, S7–S14.

44. Klimaschewski, L. (2003) Ubiquitin-dependent proteolysis in neurons. *News Physiol. Sci.*, **18**, 29–33.

45. Miller, R.J. and Wilson, S.M. (2003) Neurological disease: UPS stops delivering! *Trends Pharmacol. Sci.*, **24**, 18–23.

46. Broers, J.L., Kuijpers, H.J., Ostlund, C., Worman, H.J., Endert, J. and Ramaekers, F.C. (2005) Both lamin A and lamin C mutations cause lamina instability as well as loss of internal nuclear lamin organization. *Exp. Cell. Res.*, **304**, 582–592. Epub 2004, December 2020.

47. Lammerding, J., Schulze, P.C., Takahashi, T., Kozlov, S., Sullivan, T., Kamm, R.D., Stewart, C.L. and Lee, R.T. (2004) Lamin A/C deficiency causes defective nuclear mechanics and mechanotransduction. *J. Clin. Invest.*, **113**, 370–378.

48. Vecerova, J., Koberna, K., Malinsky, J., Soutoglou, E., Sullivan, T., Stewart, C.L., Raska, I. and Misteli, T. (2004) Formation of nuclear splicing factor compartments is independent of lamins A/C. *Mol. Biol. Cell*, **15**, 4904–4910. Epub 2004, September 4908.

49. Hutchison, C.J. (2002) Lamins: building blocks or regulators of gene expression? *Nat. Rev. Mol. Cell Biol.*, **3**, 848–858.

50. Omary, M.B., Coulombe, P.A. and McLean, W.H. (2004) Intermediate filament proteins and their associated diseases. *N. Engl. J. Med.*, **351**, 2087–2100.

51. Ostlund, C., Bonne, G., Schwartz, K. and Worman, H.J. (2001) Properties of lamin A mutants found in Emery–Dreifuss muscular dystrophy, cardiomyopathy and Dunnigan-type partial lipodystrophy. *J. Cell Sci.*, **114**, 4435–4445.

52. Raharjo, W.H., Enarson, P., Sullivan, T., Stewart, C.L. and Burke, B. (2001) Nuclear envelope defects associated with LMNA mutations cause dilated cardiomyopathy and Emery–Dreifuss muscular dystrophy. *J. Cell Sci.*, **114**, 4447–4457.

53. Reichart, B., Klafke, R., Dreger, C., Kruger, E., Motsch, I., Ewald, A., Schafer, J., Reichmann, H., Muller, C.R. and Dabauvalle, M.C. (2004) Expression and localization of nuclear proteins in autosomal-dominant Emery–Dreifuss muscular dystrophy with LMNA R377H mutation. *BMC Cell Biol.*, **5**, 12.

54. Zastrow, M.S., Vlcek, S. and Wilson, K.L. (2004) Proteins that bind A-type lamins: integrating isolated clues. *J. Cell. Sci.*, **117**, 979–987.

55. Shy, M.E., Jani, A., Krajewski, K., Grandis, M., Lewis, R.A., Li, J., Shy, R.R., Balsamo, J., Lilien, J., Garbern, J.Y. *et al.* (2004), Phenotypic clustering in MPZ mutations. *Brain*, **127**, 371–384. Epub 2004, January 2007.

56. Bouhouche, A., Benomar, A., Birouk, N., Mularoni, A., Meggouh, F., Tassin, J., Grid, D., Vandenberghe, A., Yahyaoui, M., Chkili, T. *et al.* (1999) A locus for an axonal form of autosomal recessive Charcot–Marie–Tooth disease maps to chromosome 1q21.2–q21.3. *Am. J. Hum. Genet.*, **65**, 722–727.

57. De Sandre-Giovannoli, A., Chaouch, M., Kozlov, S., Vallat, J.M., Tazir, M., Kassouri, N., Szepetowski, P., Hammadouche, T., Vandenberghe, A., Stewart, C.L. *et al.* (2002) Homozygous defects in LMNA, encoding lamin A/C nuclear-envelope proteins, cause autosomal recessive axonal neuropathy in human (Charcot–Marie–Tooth disorder type 2) and mouse. *Am. J. Hum. Genet.*, **70**, 726–736. Epub 2002, Jan 2017.

58. Tazir, M., Azzedine, H., Assami, S., Sindou, P., Nouioua, S., Zemmouri, R., Hamadouche, T., Chaouch, M., Feingold, J., Vallat, J.M. *et al.* (2004) Phenotypic variability in autosomal recessive axonal Charcot–Marie–Tooth disease due to the R298C mutation in lamin A/C. *Brain*, **127**, 154–163. Epub 2003, November 2007.

59. Sylvius, N., Bilinska, Z.T., Veinot, J.P., Fidzianska, A., Bolongo, P.M., Poon, S., McKeown, P., Davies, R.A., Chan, K.-L., Tang, A.S.L. *et al.* (2005) *In vivo* and *in vitro* examination of the functional significances of novel lamin gene mutations in heart failure patients. *J. Med. Genet.*, **42**, 639–647.

60. Evgrafov, O.V., Mersiyanova, I., Irobi, J., Van Den Bosch, L., Dierick, I., Leung, C.L., Schagina, O., Verpoorten, N., Van Impe, K., Fedotov, V. *et al.* (2004) Mutant small heat-shock protein 27 causes axonal Charcot–Marie–Tooth disease and distal hereditary motor neuropathy. *Nat. Genet.*, **36**, 602–606. Epub 2004, May 2002.

61. Cohen, M., Lee, K.K., Wilson, K.L. and Gruenbaum, Y. (2001) Transcriptional repression, apoptosis, human disease and the functional evolution of the nuclear lamina. *Trends Biochem. Sci.*, **26**, 41–47.

62. Goldman, R.D., Gruenbaum, Y., Moir, R.D., Shumaker, D.K. and Spann, T.P. (2002) Nuclear lamins: building blocks of nuclear architecture. *Genes Dev.*, **16**, 533–547.

63. Gruenbaum, Y., Margalit, A., Goldman, R.D., Shumaker, D.K. and Wilson, K.L. (2005) The nuclear lamina comes of age. *Nat. Rev. Mol. Cell Biol.*, **6**, 21–31.

64. Chen, L.S., Tassone, F., Sahota, P. and Hagerman, P.J. (2003) The (CGG)n repeat element within the 5′ untranslated region of the *FMR1* message provides both positive and negative *cis* effects on *in vivo* translation of a downstream reporter. *Hum. Mol. Genet.*, **12**, 3067–3074.

65. Schwartz, P.H., Bryant, P.J., Fuja, T.J., Su, H., O'Dowd, D.K. and Klassen, H. (2003) Isolation and characterization of neural progenitor cells from post-mortem human cortex. *J. Neurosci. Res.*, **74**, 838–851.

66. Garcia Arocena, D., Breece, K.E. and Hagerman, P.J. (2003) Distribution of CGG repeat sizes within the fragile X mental retardation 1 (*FMR1*) homologue in a non-human primate population. *Hum. Genet.*, **113**, 371–376.

67. LaSalle, J.M., Goldstine, J., Balmer, D. and Greco, C.M. (2001) Quantitative localization of heterogeneous methyl-CpG-binding protein 2 (MeCP2) expression phenotypes in normal and Rett syndromezbrain by laser scanning cytometry. *Hum. Mol. Genet.*, **10**, 1729–1740.